5 Land Use Land Cover Change Modeling and Future Simulation in Mumbai City by Integrating Cellular Automata and Artificial Neural Network

Mohd Waseem Naikoo, Shahfahad, Swapan Talukdar, Tanmoy Das, Mansoor Ahmad, Asif, Mohammad Ishtiaque, and Atiqur Rahman

Abstract

The rapid urbanization driven by population growth and economic development has led to a drastic transformation of urban landscape in the cities of developing countries. As a result, large-scale changes in the urban land use land cover (LULC) pattern have been noted in recent decades. The present study is intended to study the LULC changes in the financial capital of India that is Mumbai city from 1991 to 2018 as well as forecast LULC changes for 2030. The Landsat datasets has been used for the LULC mapping of 1991, 2001, 2011 and 2018. For the LULC classification, unsupervised classification has been used employing K means clustering technique. The kappa coefficient has been applied for examining the accuracy of classified LULC maps. The LULC changes have been forecasted for 2030 by integrating artificial neural networks (ANN) and cellular automata (CA). The results of the study show large-scale changes in all LULC categories. The built-up area of the Mumbai city has increased from 28 to 57% of the total area of the city from 1991 to 2018. The vegetation, crop land and open land have witnessed considerable decline in the coverage area from 1991 to 2018. The results of LULC forecasting shows that the built-up will increase from 55 to 66% of the total area in Mumbai by 2030. At the same time, the area under open land and vegetation will reduce from 10.26 to 3.79% and 23.33 to 21.19%, respectively, by 2030. The finding of this study may be utilized in the urban planning of Mumbai city and its adjacent areas.

Keywords

Land use land cover (LULC) · K means clustering · Cellular automata · Artificial neural network · Built-up expansion · Mumbai city

5.1 Introduction

The process of urbanization is rapidly changing the landscape in the developing countries with higher concentration of population settling in the urban areas (Zhongming et al. 2020). This urbanization is mainly driven by the economic development, increased employment opportunities and

M. W. Naikoo · Shahfahad · S. Talukdar · T. Das · Asif · M. Ishtiaque · A. Rahman (✉)
Department of Geography, Faculty of Natural Sciences, Jamia Millia Islamia, New Delhi 110025, India
e-mail: arahman2@jmi.ac.in

M. Ahmad
Department of Geography, University of Jammu, Jammu, Jammu and Kashmir 180006, India

A. Rahman et al. (eds.), *Advancements in Urban Environmental Studies*, GIScience and Geo-environmental Modelling, https://doi.org/10.1007/978-3-031-21587-2_5

higher standards of living (Sarkar 2020; Crankshaw and Borel-Saladin 2019). The increasing concentration of population in the in urban centers results in large-scale changes in land uses in these cities (Hussain et al. 2020; Zope et al. 2016; Naikoo et al. 2022). The emerging land use patterns are characterized by the predominance of impervious surfaces and declining concentration of vegetation and crop land (Naikoo et al. 2020). The increased proportion of impervious surfaces has resulted in various environmental problems like urban heat island (Mallick et al. 2013), decline in urban landscape quality (Kumari et al. 2019), water logging (Zhang et al. 2016), decline in groundwater quality and quantity (Roy et al. 2020; Lorenzen et al. 2012), increase in urban crime (Patil and Sharma 2020), etc. Thus, mapping and monitoring of urban land use land cover (LULC) changes and urban growth are highly required in the developing cities of the world.

Remote sensing and geographical information system (GIS) have been successfully used in mapping the features as well as processes taking place on the surface of earth (Wentz et al. 2014; Chaminé et al. 2021). One of the most important and frequently used application of remote sensing and GIS is the mapping of changes taking place in LULC over the surface of earth (Dewan and Yamaguchi 2009). Different methodologies have been used for classification of LULC including maximum likelihood classification, K means clustering as well as machine learning algorithms (Talukdar et al. 2020; Wang and Maduako 2018). In the present study, K means clustering technique has been used for the LULC classification. The K means clustering has been commonly used to classify LULC in the Indian cities. Naikoo et al. (2020) used K means clustering for LULC classification of Delhi NCR and reported an accuracy level of more than 85%. Similarly, Viana et al. (2019) used K means clustering in Portugal for LULC classification with an overall accuracy level in excess of 80%. Several methodologies have also been developed and applied for the LULC probabilities as well as forecasting (Das et al. 2022; Singh et al. 2015). Important methodologies for LULC forecasting include cellular automata, SLEUTH model, artificial neural networking, random forest model, Markov chain, agent-based models, etc. (Aburas et al. 2017). The application of these methodologies depends upon the availability of data and the objective of the study (Tripathy and Kumar 2019).

The Indian cities are witnessing large-scale changes in the redistribution of population due to rapid urbanization in last few decades with more population concentrating in the urban areas (Ahluwalia et al. 2014). As a result, the Indian cities are subjected to fast built-up expansion resulting in various issues like urban sprawl, congestion, environmental issues like UHI, pollution, loss of ecosystem services, etc., leading to unsustainable urban development (Gumma et al. 2017; Shahfahad et al. 2022; Das and Das 2019). Therefore, monitoring the LULC changes and built-up expansion is essential for sustainable growth of Indian cities. Studies have been done to monitor the LULC changes in the metropolitan cities of Indian including Delhi (Naikoo et al. 2020), Mumbai (Shahfahad et al. 2021), Chennai (Mathan and Krishnaveni 2020) and Kolkata (Mondal et al. 2016). In the context of Mumbai city, studies have been done to quantify the LULC changes (Shahfahad et al. 2021; Jain et al. 2021; Rahaman et al. 2021) however, none of these studies have analyzed sub-district-wise changes in LULC patterns and forecasted LULC patterns. Therefore, the present study is intended to assess the LULC changes in Mumbai city as well as forecast the same for 2030 using ANN based cellular automata.

5.2 Materials and Methods

5.2.1 Study Area

Mumbai is located at the western coast of India and is the largest metropolitan city in India in terms of population. Mumbai lies between 72° to 72°59′ E longitude and 18°53′ to 19°16′ N latitude spreading over 603 km^2 (Fig. 5.1). The city has a tropical moist type climate with mean annual rainfall above 250 cm (1901–2015) with higher concentration in the months of June to August

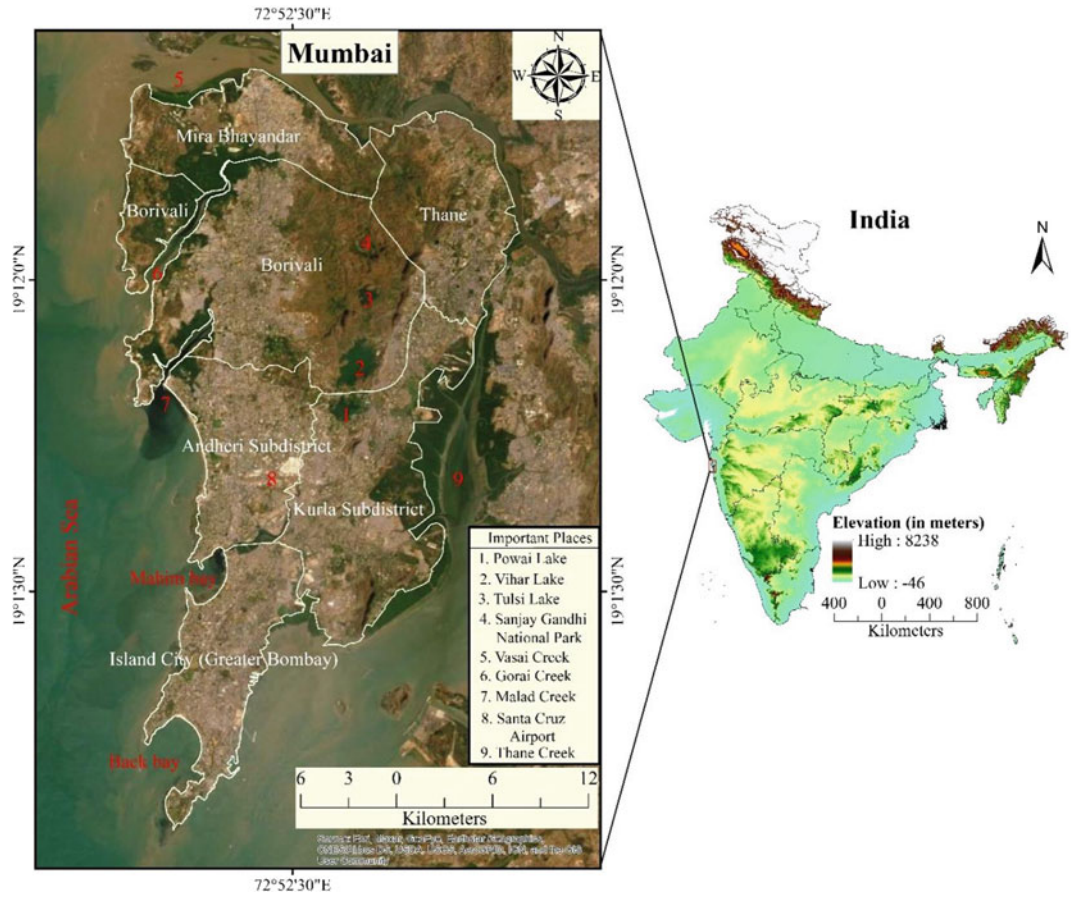

Fig. 5.1 Location of the study area

(Roy and Balling 2005). Mumbai city has an average relative humidity ranging from 54.5 to 85.5% (Rahaman et al. 2021). The Mumbai city has experienced rapid growth in population in recent decades due to higher financial prospects of the city. Mumbai city has witnessed rapid growth of population which has resulted in the degradation of environment leading to several eco-environmental problems in the city (Sarkar et al. 2020). According to the Mumbai Metropolitan Region Development Authority (MMRDA) report, nearly 5 million new housing units will be required to accommodate the increasing population of the city by 2022 (MMRDA 2016). Thus, the built-up area is expected to increase manifolds in coming decades.

5.2.2 Materials Used

The study is based on Landsat data downloaded from USA geological survey (USGS) website. Landsat (TM, ETM and OLI) data has been used for the year 1991, 2001, 2011 and 2018 to get the LULC classified images as well as for forecasting. The shapefile for Mumbai has been obtained from survey of India toposheet at a scale of 1:25,000. For LULC forecasting, eight conditioning variables have been used including elevation, slope, aspect, distance from built-up area, distance from water bodies, distance from vegetation, distance from transport network and population. The details of these conditioning variables have been presented in Table 5.1.

Table 5.1 Details of the satellite datasets used

Data	Criteria	LULC simulation	Description	Source	Year
DEM	Elevation	Conditioning parameters	SRTM DEM, 30-m resolution	https://earthexplorer.usgs.gov/	2014
	Slope	Conditioning parameters	SRTM DEM, 30-m resolution	https://earthexplorer.usgs.gov/	2014
	Aspect	Conditioning parameters	SRTM DEM, 30-m resolution	https://earthexplorer.usgs.gov/	2014
LULC	LULC	Input data	Landsat (TM, ETM+ & OLI)	https://earthexplorer.usgs.gov/	1991, 2001, 2011 & 2018
	Distance from built-up area	Conditioning parameters	Landsat (TM, & OLI)	https://earthexplorer.usgs.gov/	2011 & 2018
	Distance from vegetation	Conditioning parameters	Landsat (TM, & OLI)	https://earthexplorer.usgs.gov/	2011 & 2018
	Distance from water bodies	Conditioning parameters	Landsat (TM, & OLI)	https://earthexplorer.usgs.gov/	2011 & 2018
Transport network	Distance from Transport Network	Conditioning parameters	Major and minor roads	http://www.diva-gis.org/gdata	2011
Population	Population	Conditioning parameters	Grid-wise Population data	–	2011
City shapefile	City boundary	Input data	City boundary of Mumbai city	Survey of India Toposheet	2005

5.2.3 Methods

The present study is intended to study the LULC changes in Mumbai city as well as forecast its changes for 2030. For this purpose, satellite data has been used for LULC classification using unsupervised method. Further, with the help conditioning variables and ANN-based cellular automata, LULC changes have been simulated for 2030. The details of the methodology are presented in Fig. 5.2.

5.2.3.1 Satellite Data Pre-processing

The satellite data was downloaded from the Earth Explorer website of USGS, and then atmospheric and radiometric corrections were done to increase the image quality for easy interpretation and analysis. Various image correction and enhancement techniques available include haze and noise reduction, histogram equalization, filtering, image fusion, etc. (Lu and Weng 2007). In the present study, the layer staked images were subjected to atmospheric and radiometric correction including image fusion, haze and noise reduction as well as histogram equalization. Besides all the condition variables were resampled to fit the scale of the input parameters to that of LULC images.

5.2.3.2 LULC Classification and Accuracy Assessment

There are several methods for carrying out LULC classification including Iterative Self-Organizing Data Analysis Technique (ISODATA), K means clustering, etc. (Goncalves et al. 2008). In this study, LULC classification has been carried out

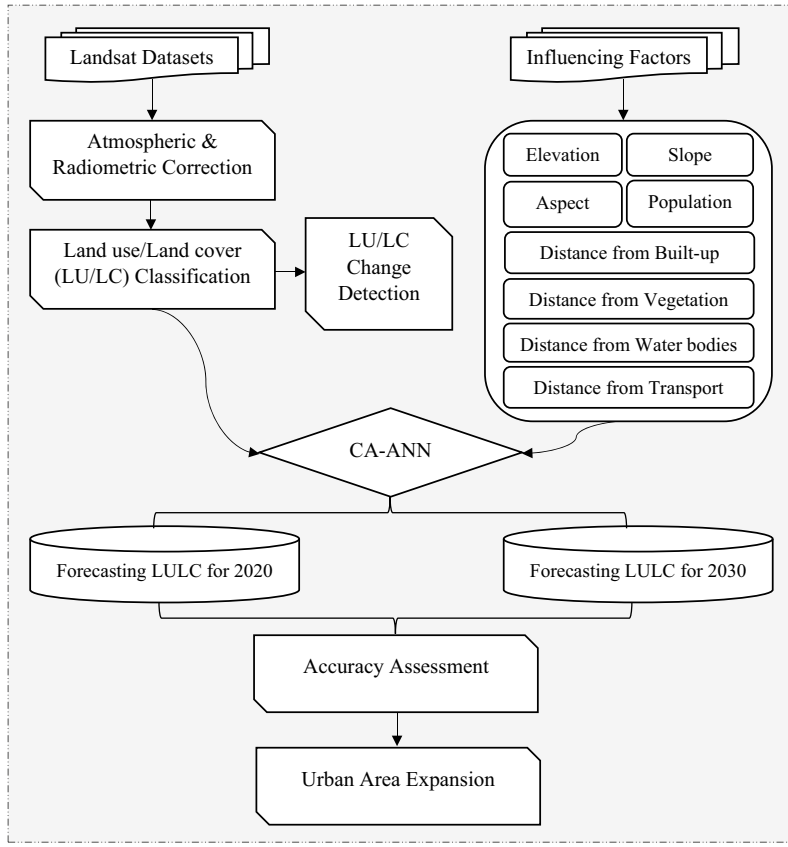

Fig. 5.2 Flowchart of the methodology

using K means clustering method in ERDAS Imagine software. K means clustering divides *m* number of observations on a m dimensional surface into k clusters (Gupta and Venkatesan 2020). A total of six major LULC classes have been identified in Mumbai, i.e., built-up, cropland, open land, water body, dense vegetation (forest) and sparse vegetation (scrubland) based on NRSC level I classification scheme. The identified classes were validated by field visits and the using GPS. Finally, LULC change was estimated using multi-temporal raster layers for 1991, 2001, 2011 and 2018 and comparing their corresponding statistics.

5.2.3.3 Preparation of the Conditioning Parameters for Future LULC Simulation

For simulation of LULC, some independent parameter needs to be identified that can explain the growth of LULC changes over time. Hence, in this study, eight conditioning parameters have been identified namely elevation, slope, aspect, distance to waterbody, distance to built-up area, population and distance to transportation network (Fig. 5.3). Physical factors, i.e., elevation, slope and aspects, are considered as important factors that determine the LULC change (Birhane et al. 2019). Elevation, slope and aspect have been derived from Advanced Land Observing Satellite (ALOS) Polarimetric Phased Array L-band Synthetic Aperture Radar (PALSAR) digital elevation model. The population data has been taken from gridded population data taken from Socioeconomic Data and Applications Center (SEDAC) website hosted by Center for International Earth Science Information Network (CIESIN) at Columbia University. Population growth is the primary cause leading to the changes in LULC changes. Euclidian distance has been used to obtain the distance to built-up area, vegetation and water bodies from LULC images.

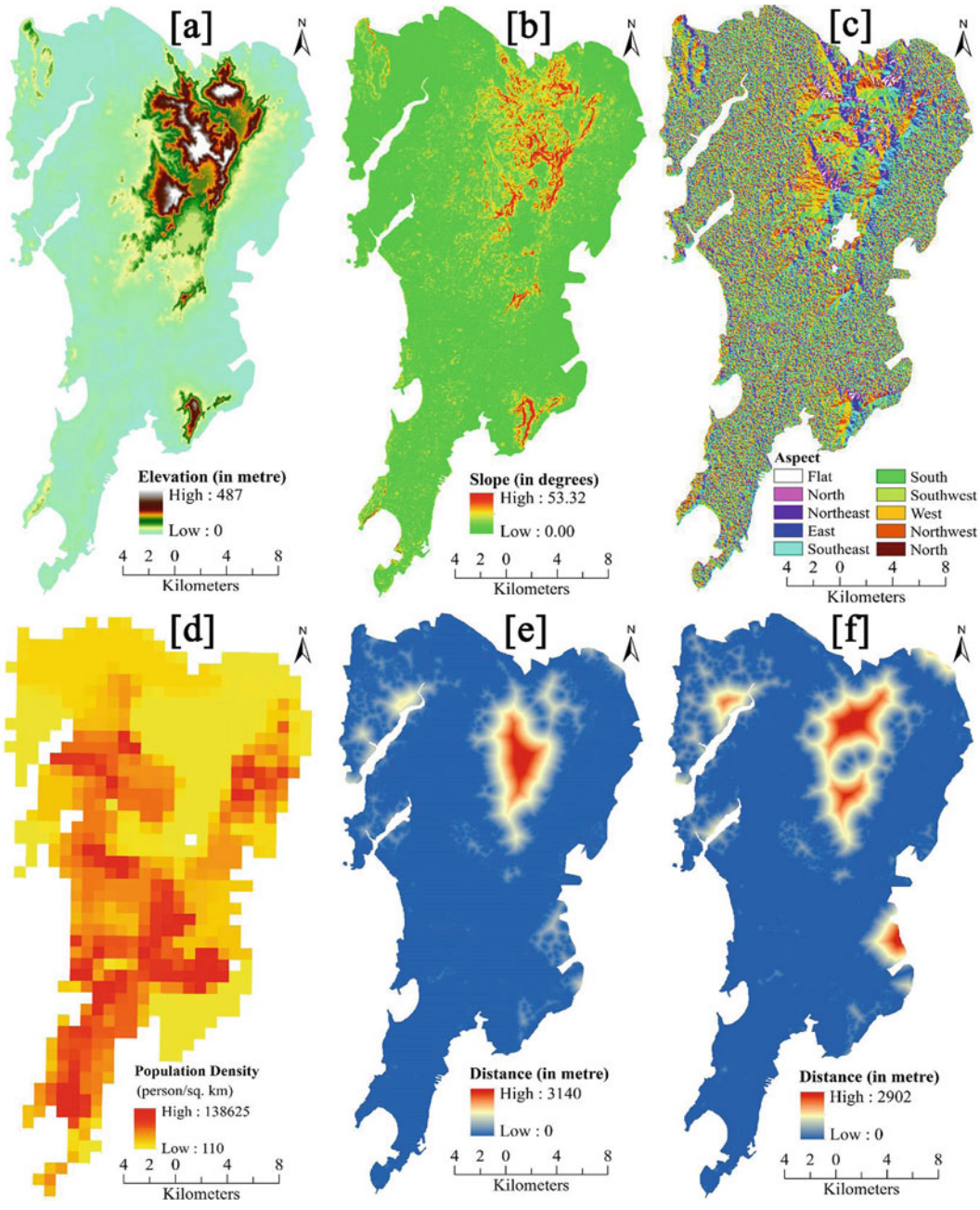

Fig. 5.3 LU/LC simulation conditioning parameters **a** elevation, **b** slope, **c** aspect, **d** population, **e** distance from built-up area 2011, **f** distance from built-up area 2018, **g** distance from transport network, **h** distance from vegetation 2011, **i** distance from vegetation 2018, **j** distance from water bodies 2011 and **k** distance from water bodies 2018

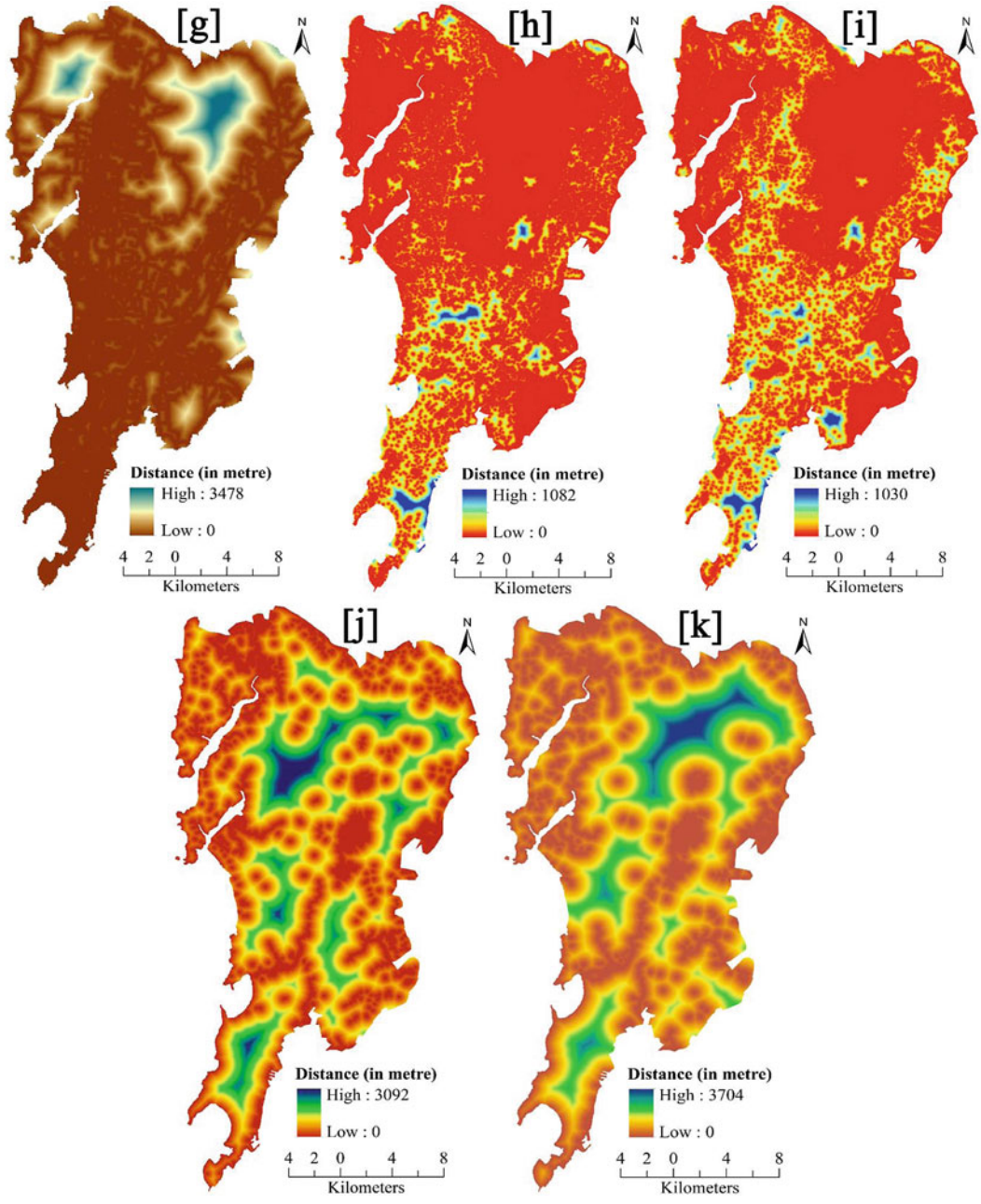

Fig. 5.3 (continued)

5.2.3.4 Simulation of Future LULC Pattern

The LULC changes have been simulated for 2030 using artificial neural network (ANN)-based cellular automata (CA). ANN estimates LULC transformation probabilities using multiple output neurons by simulating several LULC changes. The transition probabilities learnt from ANN learning process are used by the CA to simulate LULC changes (Saputra and Lee 2019). The CA-ANN model was applied in six steps using QGIS open-source software version 3.22.

In the first step, the input layers of neural network are defined to simulate the future LULC changes. The simulation process executes at pixel level, in which each pixel in the neural network gets input from *n*-attributes. The attributes in the neural network can be estimated using Eq. 5.1.

$$X = [x_1, x_2, x_3, \ldots\ldots\ldots, x_n]^{\mathrm{T}} \quad (5.1)$$

where x_1, x_2, x_3 are attributes, and T represents the transposition. In this step, the LULC maps of 1991, 2001, 2011 and 2018 along with all conditioning variables are used as input layers. These conditioning variables were resampled at 30 m resolution in raster format to match the resolution with the LULC images and for obtaining the attributes. In the second step, correlation between the conditioning variables was ascertained by two-way raster comparison, in which first raster is selected from one variable, while second raster is selected from different variables. Further, in this step, the change in area from starting raster to final raster is calculated, and transition matrix for the proportion of changed pixels was calculated.

In third step, transition probabilities were modeled using ANN. The structure of neural network is made up of three layers input layer, hidden layer and output layer. The input layer involves the resampling of each variable into 0 and 1, and each variable gets associated with a neuron. In hidden layer, the signal received by any neuron from input layer at any time is given by Eq. 5.2.

$$\mathrm{net}_j(k,t) = \sum\nolimits_i w_{i,k} x_i'(k,t) \quad (5.2)$$

where $w_{i,k}$ describes the weight between the input and hidden layers; x_i' refers to the i scaled attribute which is associated with the neuron i in the input layer related to the k-th cell at time t. A total of 12 neurons have been used to get perfect fit of a continuous function in the neural networks. The output layer has 6 neurons which corresponds to the 6 LULC classes. Further, the neuron m in the output layer generates a value which represents the transition probabilities from original LULC type m. The transition probability is calculated as per the output function in the neural network given by Eq. 5.3.

$$P(k,t,m) = \sum\nolimits_j w_{j,m} \frac{1}{i + e - \mathrm{net}_j(k,t)'} \quad (5.3)$$

where $P(t,\ k,\ m)$ represents the possibility of conversion to *m-class* LULC at time t for the cell k, while $w_{j,1}$ refers to the refers to the weight between hidden layer and output layers.

The fourth step involves applying the CA model to simulate LULC change. The CA is made up of regular spatial grids of cells that can be used in any number of states, depending on the states of surrounding cells. It evaluates the structure of cell connections in the vicinity of a single cell. The validation of simulated LULC maps was completed in next step, followed by a comparison of the simulated and original LULC maps from 2018. Finally, following confirmation, the LULC projection for 2018 was made based on the assumption that the current LULC change pattern will continue.

5.3 Results and Discussion

5.3.1 LULC Pattern During 1991–2018

The LULC pattern for Mumbai city from 1991 to 2018 has been divided into six categories including built-up area, crop land, dense vegetation, sparse vegetation, water bodies and open land (Fig. 5.4). For LULC classification, K means clustering has been used which is simple and easy to execute and has been successfully used by several studies as well (Naikoo et al. 2020; Viana et al. 2019). In Mumbai city, the built-up area is mostly concentrated in the southern peninsular parts of the city in 1991. The prominence of built-up area increases in the subsequent time periods toward the western and eastern parts of the city. In 2018, with the exception of the central region of city and small

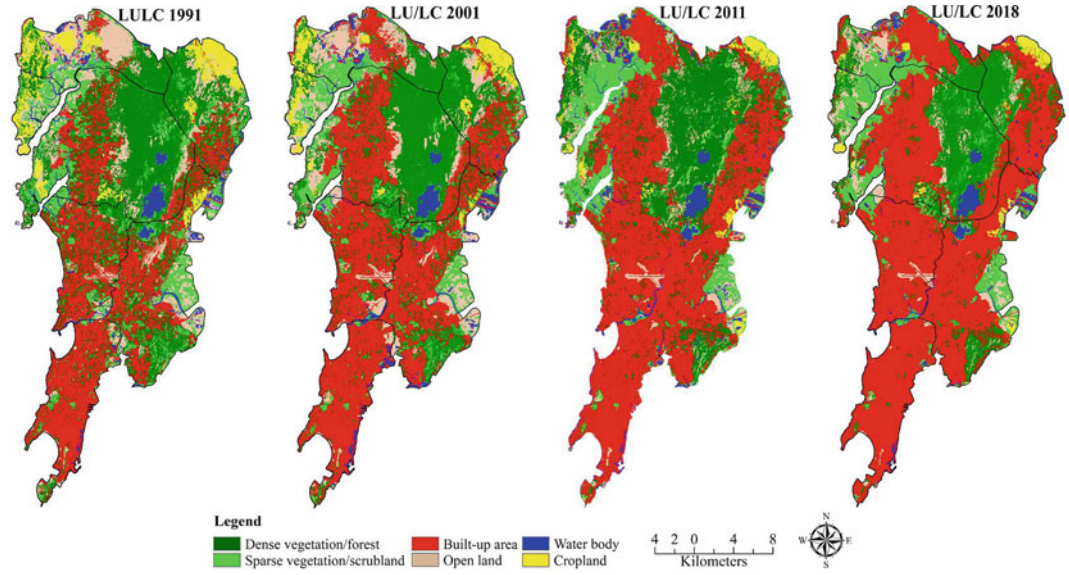

Fig. 5.4 Land use/land cover (LU/LC) pattern of Mumbai city during 1991–2018

portions in NW and SE, entire landscape is covered by built-up area. Thus, in Mumbai, the built-up area increased both in core (peninsular part) and other peripheral parts. Previously, studies have shown the infilling in the core due to continues migration and population growth in cities (Yang et al. 2018). Further, the expansion of built-up area into the peripheries of core is occurring due to congestion in the core region (Güneralp et al. 2020). Dense vegetation is present in the central region of the city and in patches in the eastern and western stretches of the city. Over time, there is little change in the homogeneity of the dense vegetation in the central region but its presence in other parts of the city diminishes considerably. Cropland is present on the extreme NW and NE of the Mumbai city in 1991, and over time, the agricultural land on the NE declined considerably, while on the NW, it disappeared in 2018.

In 1991, the maximum area of Mumbai city was under vegetation (215 km^2), and minimum was under water bodies (27.19 km^2), while the area under built-up area was only 173 km^2 (Table 5.2). Over all, the maximum percentage area was under vegetation (35%) followed by built-up area (28%) and minimum area was under water bodies (4.50%) and crop land (5.82%) in 1991. In 2001, the percentage area under built-up was 40% which increased up to 49% in 2011 and 57% in 2018. Similarly, the percentage area under crop land was about 3% in 2001, 2.46% in 2011 and 1.71% in 2018. The percentage area under scrubland was about 11.93% in 1991, 9.45% in 2001, 11.08% in 2011 and 10.61% in 2018. In 1991, open land occupied 13.34% area in 1991, 11.69% in 2001, 6.58% in 2011 and 5.59% in 2018. In 2018, the area was maximum under built-up (346 km^2) followed by vegetation (21%), while the area was minimum under crop land (10.32 km^2). In terms of percentage, the maximum area was under built-up area (about 57%) followed by vegetation cover (21%) and scrubland (10.61%), while open land (5.59%) and water bodies (3.36%) had very low percent of area under it.

The city of Mumbai is divided into six sub-districts namely Greater Mumbai, Andheri, Borivali, Kurla, Thane and Mira Bhayandar. Among the sub-districts, the built-up area is maximum in greater Bombay with value ranging from 71km^2 in 1991 to 91km^2 2018 (Fig. 5.5).

Table 5.2 Land use land cover (LULC) change in Mumbai city during 1991–2018

LU/LC class	1991		2001		2011		2018	
	Area in km^2	Area in percent	Area in km^2	Area in percent	Area in km^2	Area in percent	Area in km^2	Area in percent
Built-up area	173.09	28.67	247.09	40.90	296.79	49.16	346.02	57.31
Open land	80.57	13.34	70.16	11.69	39.74	6.58	33.78	5.59
Vegetation	215.8	35.74	179.48	29.71	159.05	26.34	129.27	21.41
Scrubland	71.96	11.93	57.18	9.46	66.87	11.08	64.08	10.61
Cropland	35.17	5.82	23.47	3.88	14.86	2.46	10.32	1.71
Water bodies	27.19	4.50	26.40	4.36	26.47	4.38	20.31	3.36
Total	603.78	100	603.78	100	603.78	100.00	603.78	100.00

The built-up area is minimum in Mira Bhayandar in 1991 (6.59%), while in 2018, it is minimum in Borivali (37.11km^2). The area under open land is maximum in Mira Bhayandar which constitutes about 32.1% in 1991 and 12% of the total open area of the city in 2018. The open area is minimum in greater Bombay constituting about 4% in 1991 and 1.82% of the total open area of the city in 2018. Dense vegetation is maximum in Borivali making up to 34% of the total area under dense vegetation in 2018. Similarly, Borivali has the maximum area under scrubland constituting to about 12% in 1991 and 15% of the total area under scrubland in 2018. In 1991, the area of crop land is maximum under Mira Bhayandar (15.5%), while in 2018, it is maximum in Kurla (2.22%). The area under water bodies is maximum in Borivali throughout the study time. Thus, maximum area under dense vegetation, scrubland and water bodies is found in Borivali sub-district of Mumbai city.

5.3.2 LU/LC Change During 1991–2018

The transformation of one LULC class into another in Mumbai city has been presented in Fig. 5.6 and Table 5.3. The built-up area expansion of about 350 km^2 has come mostly at the cost of vegetation (96.6 km^2), open land (41 km^2), scrubland (22 km^2) and crop land (12.35 km^2). The expansion of built-up area at the expense of vegetation, open land and scrubland has been reported in several parts of the globe (Nong et al. 2018; Spyra et al. 2021; Naikoo et al. 2023). Vegetation has witnessed a maximum decline up to 129 km^2 and has been transformed mostly into scrubland (13.18 km^2), open land (7.86 km^2), crop land (7.1 km^2) and built-up area (2.47 km^2). However, the area under scrubland has declined marginally by 7 km^2. The scrubland got converted into in to built-up area (22.25 km^2), vegetation (13.18 km^2) and open land (3.06 km^2). At the same time, the scrubland increased it area from open land (16.21 km^2) and water body (5.1 km^2). In Mumbai city, the open land has been converted into built-up (41 km^2), scrubland (16.21 km^2) and vegetation (7.86 km^2). Crop land was converted into built-up area (12.35 km^2) and open land (7.45 km^2).

5.3.3 Sub-district-Wise Change in LU/LC Pattern

The heat-map prepared using R Studio software package shows LULC changes in the sub-district of Mumbai city during 1991–2018 (Fig. 5.7). The analysis of figure shows that the built-up area has increased in the all the sub-districts of Mumbai city. At the same time, the scrublands, open land and vegetation cover had experienced

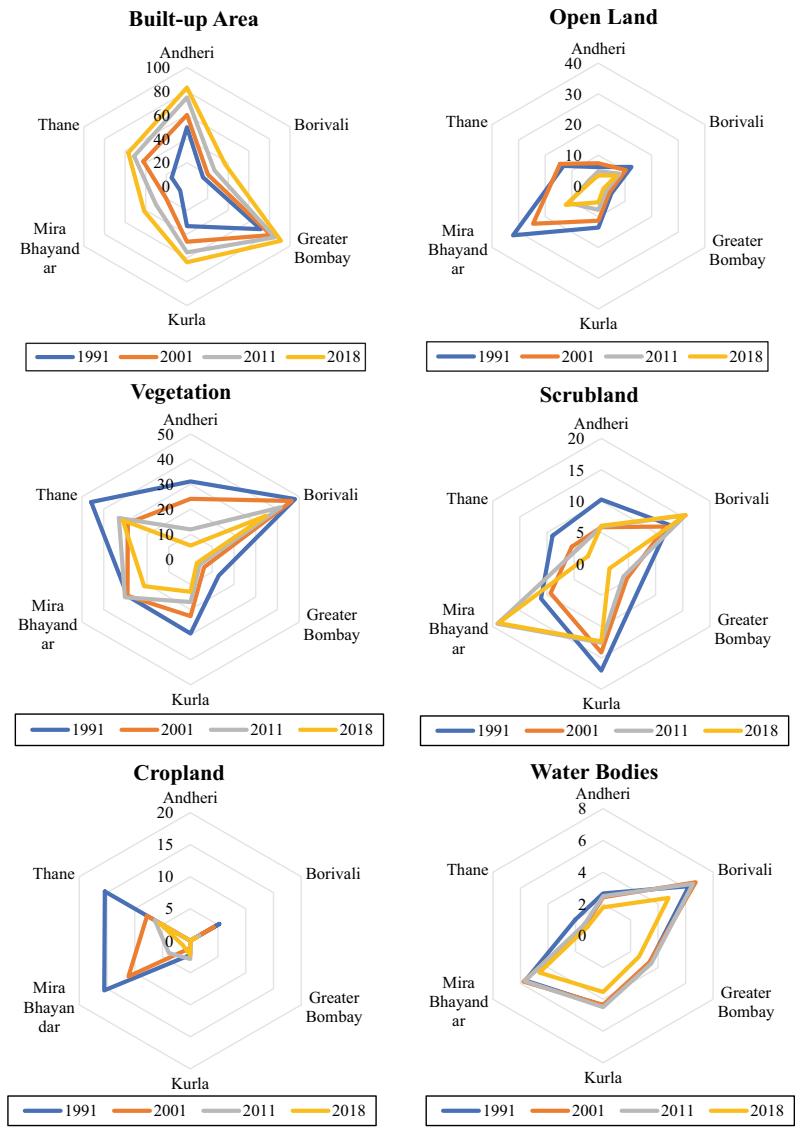

Fig. 5.5 Sub-district-wise variation in LU/LC pattern in Mumbai city during 1991–2018

consistent decline. Overall, the maximum change has been noticed from the vegetation cover, open land and built-up area. Studies shows that in the process of urbanization, the built-up areas expand mostly at the expense of vegetation cover, cropland and open land (Borrelli et al. 2020). However, in Mumbai city, the cropland was present in very low proportion in 1991 which has been declined to almost half of its total area during 1991–2018. Contrary to this, the vegetation cover had the maximum areal coverage in 1991 with 215.18 km^2 area under it which had declined to 129.27 km^2 in 2018. Shahfahad et al. (2021) reported a similar result for LULC changes in Mumbai city. During 1991–2018, while open land has seen the greatest reduction in Andheri and Kurla sub-districts, the greatest decline in vegetation cover was seen in Andheri and Mira Bhayandar sub-districts. However, the built-up area had increased in all the sub-districts with a consistent rate during 1991–2018.

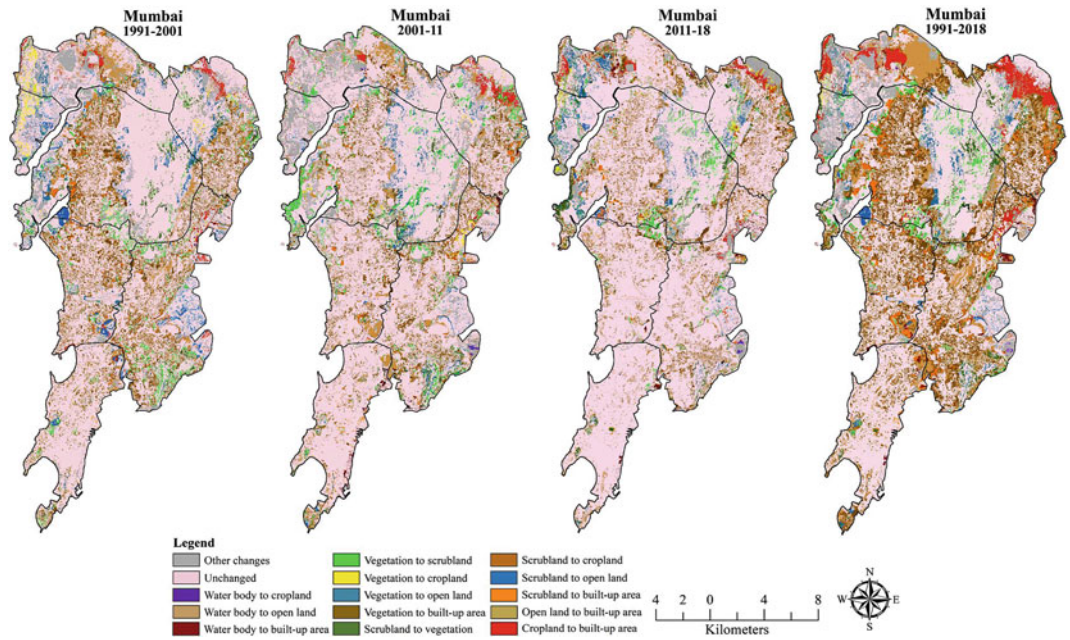

Fig. 5.6 LU/LC change in Mumbai city during 1991–2018

5.3.4 Analysis of Classification Accuracy

The accuracy assessment is a critical exercise in post classification analysis of LULC mapping. The accuracy assessment of the LULC has been assessed with the help of Kappa coefficient employing users' accuracy, producer accuracy and overall accuracy. User's accuracy for all the classified maps is over 78% with highest user's accuracy in case of 2018 (93.17%) and 2011 (93.02%). Similarly, the producer's accuracy ranges from 75% (2030) to 93.49% (2018). The overall accuracy of the LULC maps is maximum in 2018 with a value of 93% followed by 2011 with 92.80% accuracy. The overall accuracy is minimum in 2030 with a value of 76.63% (Table 5.4).

5.3.5 Analysis of Simulated LU/LC for 2020 and 2030

The LULC simulation has been done in two steps. The conditioning variables of 2011 have been used to simulate LULC change for 2020 in the first step. This simulated LULC was cross checked with the actual LULC of 2018. Once the similarity was established between simulated LULC for 2020 and actual 2018 through visualization, the second step was proceeded. In this step, the conditioning variables of 2020 have been used to forecast LULC changes for 2030 using ANN-based cellular automata. The cellular automata has been preferred for LULC furcating because it not only predicts the futuristic changes in LULC but also takes into account the influence of each conditioning factors (Wu et al. 2022). The forecasted LULC of 2030 shows a further expansion of built-up area especially in the NW and SE of the study area (Fig. 5.8).

The area under different LULC categories for simulated 2020 and forecasted 2030 has been presented in Table 5.5. Table 5.5 shows that maximum area of 332 km^2 is under built-up in 2020, while minimum area is under crop land (24.61 km^2). Similarly in forecasted 2030, built-up area further increases to 400 km^2 while crop land is reduced to only 2.86 km^2. With the exception of built-up area, all other LULC

Table 5.3 LU/LC transition matrix

LU/LC classes	Water body	Cropland	Scrubland	Vegetation	Built-up area	Open land
1991–2001 (*in* km^2)						
Water body	17.94	0.06	3.29	0.41	1.5	2.47
Crop land	0.12	18.18	1.25	5.63	2.52	9.45
Scrubland	2.22	0.31	36.73	15.79	10.1	8.2
Vegetation	0.5	2.62	8.02	137.56	54.27	12.69
Built-up area	1.86	0.08	1.22	9.93	159.22	1.67
Open land	3.46	2.21	6.5	10.12	20.43	39.62
2001–2011 (*in* km^2)						
Water body	18.37	0.39	2.08	0.39	3	1.06
Crop land	0.11	9.45	1.53	7.14	3.57	1.64
Scrubland	1.9	0.69	37.11	8.61	6.21	2.05
Vegetation	0.84	1.31	11.97	115.21	40.07	9.98
Built-up area	1.51	0.81	3.07	14.78	225.68	2.13
Open land	3.62	2.2	12.12	14.92	18.27	22.86
2011–2018 (*in* km^2)						
Water body	16.04	0.22	2.85	0.67	4.08	2.52
Crop land	0.18	8.17	0.94	1.16	2.81	1.58
Scrubland	0.64	0.28	46.66	10.48	7.39	2.43
Vegetation	0.34	1.43	6.79	103.04	38.16	11.29
Built-up area	1.76	0.19	2.7	7	283.96	1.16
Open land	0.8	0.02	5.65	6.85	9.36	17.06
1991–2018 (*in* km^2)						
Water body	13.51	0.19	5.1	0.56	4.91	1.37
Crop land	0.31	7.48	2.45	7.1	12.35	7.45
Scrubland	1.76	0.5	32.48	13.18	22.25	3.06
Vegetation	0.73	0.63	8.8	98.1	96.6	10.81
Built-up area	1.24	0.09	1.02	2.47	168.56	0.61
Open land	2.72	1.43	16.21	7.86	41.34	12.81

categories are expected to witness a decline in coverage area in 2030. The maximum decline is expected in open land whose coverage area is reduced from 61 to 22.91 km^2 only from 2020 to 2030.

5.4 Conclusion

The study has been done to analyze and forecast the spatio-temporal LULC pattern in Mumbai city using Landsat datasets. For forecasting of LULC changes for 2030, ANN integrated with CA has been used. The study's findings indicate that the built-up area has grown from 28% to the 57% of the total area of the city from 1991 to 2018. While, the vegetation, open land and crop land have declined from 35, 13.34 and 5.582% in 1991 to corresponding values of 21.41, 5.59 and 1.71% in 2018. Further, built-up area is expected to increase up to 66% of the total area of the city by 2030 as shown by the LULC simulations. The built-up area in Mumbai has expanded mostly on vegetation and open land. Among the sub-

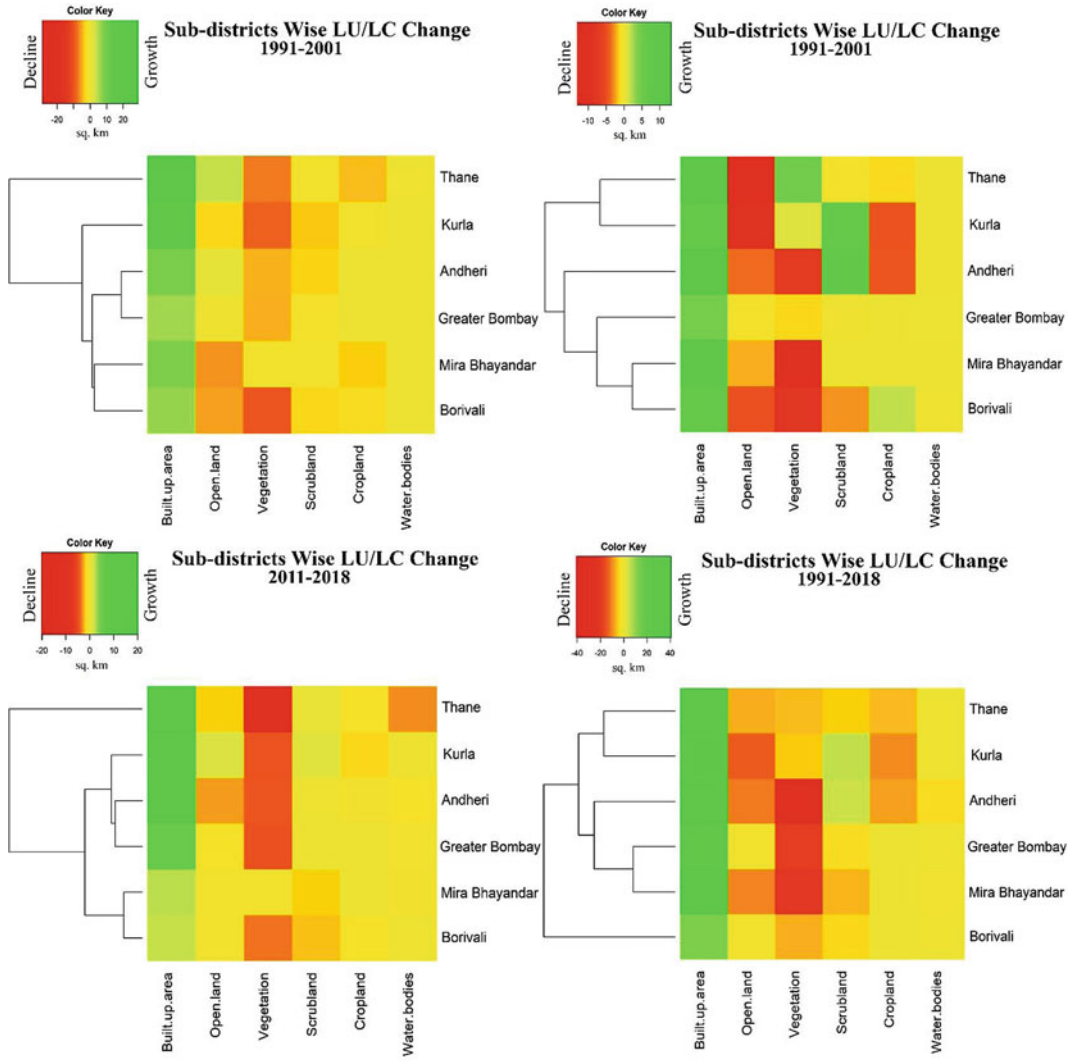

Fig. 5.7 Sub-district-wise LU/LC change in Mumbai city during 1991–2018

Table 5.4 Accuracy assessment of LU/LC maps using Kappa coefficient

Year	User's accuracy (%)	Producer's accuracy (%)	Overall accuracy (%)	Kappa coefficient
1991	88.23	88.71	87.20	0.883
2001	87.42	87.08	85.80	0.879
2011	93.02	93.05	92.80	0.941
2018	93.17	93.49	93.01	0.957
2020	86.32	85.18	85.12	0.824
2030	78.52	75.25	76.63	0.754

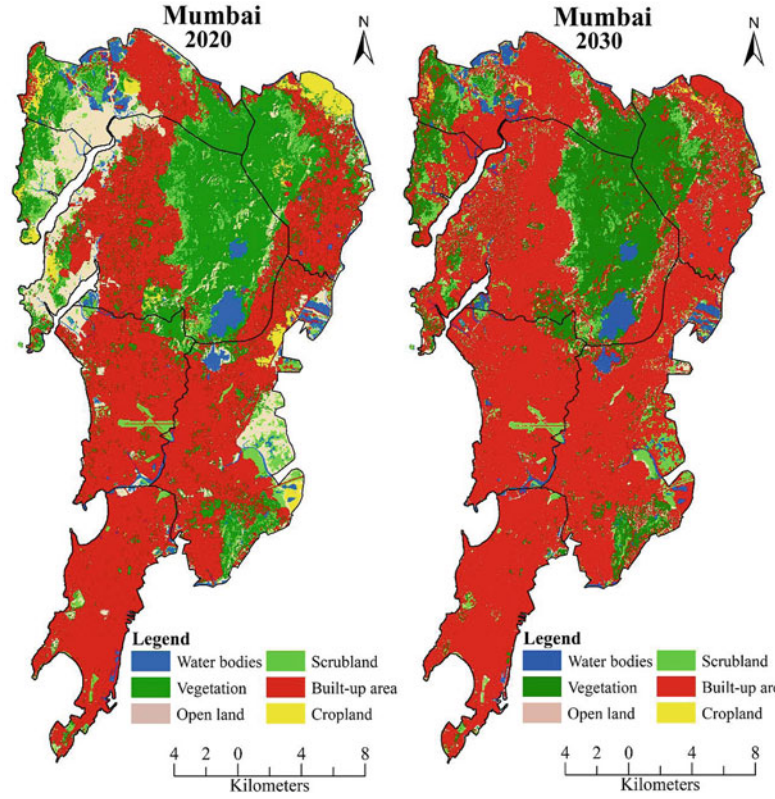

Fig. 5.8 Simulated LU/LC pattern of Mumbai for the year 2020 and 2030

Table 5.5 Area under simulated LU/LC types in Mumbai for 2020 and 2030

Class	2020		2030	
	Are in km^2	Area in percent	Are in km^2	Area in percent (%)
Water bodies	24.61	4.08	20.88	3.46
Vegetation	140.88	23.33	127.95	21.19
Open land	61.96	10.26	22.91	3.79
Scrubland	29.28	4.85	28.72	4.76
Built-up area	332.93	55.14	400.46	66.33
Crop land	14.12	2.34	2.86	0.47
Total	603.78	100.00	603.78	100.00

districts, the built-up area has increased in all the sub-districts. However, Andheri and Mira Bhayandar sub-district has seen the maximum reduction in vegetation cover, while open land had witnessed maximum decline in Andheri and Kurla sub-districts. Moreover, the vegetation cover, scrubland and open land are expected to decline significantly, mostly in the northern sub-districts like Mira Bhayandar and Thane. However, water bodies did not show a significant change in near future because most of the water bodies in Mumbai city is either protected or in the form of rivers and bays. The finding of the study that the process of urbanization leading to LULC changes has been taking place at a rapid pace and is expected to increase further in near future. Thus, there is an urgent need for the regulation and planning of the LULC changes

taking place in Mumbai city. Further research in this direction can be directed toward finding the local underlying factors leading to LULC changes as well as simulation can be done for longer time period using other methodologies like CA Markov and CA integrated machine learning algorithms.

References

Aburas MM, Ho YM, Ramli MF, Ash'aari ZH (2017) Improving the capability of an integrated CA-Markov model to simulate spatio-temporal urban growth trends using an Analytical Hierarchy Process and Frequency Ratio. Int J Appl Earth Obs Geoinf 59:65–78

Ahluwalia IJ, Kanbur R, Mohanty PK (eds) (2014) Urbanisation in India: challenges, opportunities and the way forward. SAGE Publications India

Birhane E, Ashfare H, Fenta AA, Hishe H, Gebremedhin MA, Solomon N (2019) Land use land cover changes along topographic gradients in Hugumburda national forest priority area, Northern Ethiopia. Remote Sens Appl Soc Environ 13:61–68

Borrelli P, Robinson DA, Panagos P, Lugato E, Yang JE, Alewell C, Wuepper D, Montanarella L, Ballabio C (2020) Land use and climate change impacts on global soil erosion by water (2015–2070). Proc Natl Acad Sci 117(36):21994–22001

Census of India (2011) Mumbai (Greater Mumbai) City Census 2011 data. https://www.census2011.co.in/census/city/365-mumbai.html#:~:text=Aspercent20perpercent20provisionalpercent20reportspercent20of,malespercent20andpercent208percent2C522percent2C641percent20arepercent20females. Accessed on 06/05/2022

Chaminé HI, Pereira AJ, Teodoro AC, Teixeira J (2021) Remote sensing and GIS applications in earth and environmental systems sciences. SN Appl Sci 3 (12):1–3

Crankshaw O, Borel-Saladin J (2019) Causes of urbanisation and counter-urbanisation in Zambia: natural population increase or migration? Urban Stud 56 (10):2005–2020

Das M, Das A (2019) Dynamics of urbanization and its impact on urban ecosystem services (UESs): a study of a medium size town of West Bengal, Eastern India. J Urban Manag 8(3):420–434

Das T, Naikoo MW, Talukdar S, Parvez A, Rahman A, Pal S, Asgher MS, Islam ARMT, Mosavi A (2022) Analysing process and probability of built-up expansion using machine learning and fuzzy logic in English bazar, West Bengal. Remote Sens 14 (10):2349

Dewan AM, Yamaguchi Y (2009) Land use and land cover change in Greater Dhaka, Bangladesh: using remote sensing to promote sustainable urbanization. Appl Geogr 29(3):390–401

Gebeyehu MN (2019) Remote sensing and GIS application in agriculture and natural resource management. Int J Environ Sci Nat Resourc 19(2):45–49

Goncalves ML, Netto MLA, Costa JAF, Zullo Junior J (2008) An unsupervised method of classifying remotely sensed images using Kohonen self-organizing maps and agglomerative hierarchical clustering methods. Int J Remote Sens 29(11):3171–3207

Gupta P, Venkatesan M (2020) Mineral identification using unsupervised classification from hyperspectral data. In: Emerging research in data engineering systems and computer communications. Springer, Singapore, pp 259–268

Gumma MK, Mohammad I, Nedumaran S, Whitbread A, Lagerkvist CJ (2017) Urban sprawl and adverse impacts on agricultural land: a case study on Hyderabad, India. Remote Sens 9(11):1136

Güneralp B, Reba M, Hales BU, Wentz EA, Seto KC (2020) Trends in urban land expansion, density, and land transitions from 1970 to 2010: a global synthesis. Environ Res Lett 15(4):044015

Hussain S, Mubeen M, Ahmad A, Akram W, Hammad HM, Ali M, Masood N, Amin A, Farid HU, Sultana SR, Nasim W (2020) Using GIS tools to detect the land use/land cover changes during forty years in Lodhran district of Pakistan. Environ Sci Pollut Res 27(32):39676–39692

Jain S, Roy SB, Panda J, Rath SS (2021) Modeling of land-use and land-cover change impact on summertime near-surface temperature variability over the Delhi-Mumbai Industrial Corridor. Model Earth Syst Environ 7(2):1309–1319

Kumari B, Tayyab M, Hang HT, Khan MF, Rahman A (2019) Assessment of public open spaces (POS) and landscape quality based on per capita POS index in Delhi India. SN Appl Sci 1(4):1–13

Lambin EF, Helmut GJ, Lepers E (2003) Dynamics of land-use and land-cover change in tropical regions. Annu Rev Environ Resour 28(1):205–241

Lorenzen G, Sprenger C, Baudron P, Gupta D, Pekdeger A (2012) Origin and dynamics of groundwater salinity in the alluvial plains of western Delhi and adjacent territories of Haryana State India. Hydrol Process 26(15):2333–2345

Lu D, Weng Q (2007) A survey of image classification methods and techniques for improving classification performance. Int J Remote Sens 28(5):823–870

Mallick J, Rahman A, Singh CK (2013) Modeling urban heat islands in heterogeneous land surface and its correlation with impervious surface area by using night-time ASTER satellite data in highly urbanizing city Delhi-India. Adv Space Res 52(4):639–655

Mathan M, Krishnaveni M (2020) Monitoring spatio-temporal dynamics of urban and peri-urban land transitions using ensemble of remote sensing spectral indices—a case study of Chennai Metropolitan Area, India. Environ Monitor Assessm 192(1)

Mondal MS, Sharma N, Garg PK, Kappas M (2016) Statistical independence test and validation of CA Markov land use land cover (LULC) prediction results. Egypt J Remote Sens Space Sci 19(2):259–272

MMRDA (2016) Mumbai Metropolitan regional plan; MMRDA: Mumbai, India

Naikoo MW, Rihan M, Ishtiaque M (2020) Analyses of land use land cover (LULC) change and built-up expansion in the suburb of a metropolitan city: spatio-temporal analysis of Delhi NCR using landsat datasets. J Urban Manag 9(3):347–359

Naikoo MW, Rihan M, Peer AH, Talukdar S, Mallick J, Ishtiaq M, Rahman A (2022) Analysis of peri-urban land use/land cover change and its drivers using geospatial techniques and geographically weighted regression. Environ Sci Pollut Res, 1–19

Naikoo MW, Shahfahad, Talukdar S, Ishtiaq M, Rahman A (2023) Modelling built-up land expansion probability using the integrated fuzzy logic and coupling coordination degree model. J Environ Manage 325:116441. https://doi.org/10.1016/j.jenvman.2022.116441

Nong DH, Lepczyk CA, Miura T, Fox JM (2018) Quantifying urban growth patterns in Hanoi using landscape expansion modes and time series spatial metrics. PLOS ONE 13(5):e0196940. https://doi.org/10.1371/journal.pone.0196940

Patil GR, Sharma G (2020) Urban quality of life: an assessment and ranking for Indian cities. Transp Policy

Rahaman S, Jahangir S, Haque MS, Chen R, Kumar P (2021) Spatio-temporal changes of green spaces and their impact on urban environment of Mumbai, India. Environ Dev Sustain 23(4):6481–6501

Roy SS, Balling Jr RC (2005) Analysis of trends in maximum and minimum temperature, diurnal temperature range, and cloud cover over India. Geophys Res Lett 32(12)

Roy SS, Rahman A, Ahmed S, Ahmad IA (2020) Alarming groundwater depletion in the Delhi Metropolitan Region: a long-term assessment. Environ Monit Assess 192(10):1–14

Saputra MH, Lee HS (2019) Prediction of land use and land cover changes for north sumatra, Indonesia, using an artificial-neural-network-based cellular automaton. Sustainability 11(11):3024

Sarkar R (2020) Association of urbanisation with demographic dynamics in India. GeoJournal 85(3):779–803

Sarkar T, Kannaujiya S, Taloor AK, Ray PKC, Chauhan P (2020) Integrated study of GRACE data derived interannual groundwater storage variability over water stressed Indian regions. Groundw Sustain Dev 10:100376

Shahfahad, Naikoo MW, Islam ARMT, Mallick J, Rahman A (2022) Land use/land cover change and its impact on surface urban heat island and urban thermal comfort in a metropolitan city. Urban Clim 41:101052

Shahfahad, Rihan M, Naikoo MW, Ali MA, Usmani TM, Rahman A (2021) Urban Heat island dynamics in response to land-use/land-cover change in the coastal city of Mumbai. J Indian Soc Remote Sens 49 (9):2227–2247

Singh SK, Mustak S, Srivastava PK, Szabó S, Islam T (2015) Predicting spatial and decadal LULC changes through cellular automata Markov chain models using earth observation datasets and geo-information. Environ Process 2(1):61–78

Spyra M, Kleemann J, Calò NC, Schürmann A, Fürst C (2021) Protection of peri-urban open spaces at the level of regional policy-making: examples from six European regions. Land Use Policy 107:105480. https://doi.org/10.1016/j.landusepol.2021.105480

Talukdar S, Singha P, Mahato S, Pal S, Liou YA, Rahman A (2020) Land-use land-cover classification by machine learning classifiers for satellite observations—a review. Remote Sens 12(7):1135

Tripathy P, Kumar A (2019) Monitoring and modelling spatio-temporal urban growth of Delhi using cellular automata and geoinformatics. Cities 90:52–63

Viana CM, Girão I, Rocha J (2019) Long-term satellite image time-series for land use/land cover change detection using refined open source data in a rural region. Remote Sens 11(9):1104

Wang J, Maduako IN (2018) Spatio-temporal urban growth dynamics of Lagos metropolitan region of Nigeria based on hybrid methods for LULC modeling and prediction. Eur J Remote Sens 51(1):251–265

Wentz EA, Anderson S, Fragkias M, Netzband M, Mesev V, Myint SW, Quattrochi D, Rahman A, Seto KC (2014) Supporting global environmental change research: a review of trends and knowledge gaps in urban remote sensing. Remote Sens 6 (5):3879–3905

Wu X, Liu X, Zhang D, Zhang J, He J, Xu X (2022) Simulating mixed land-use change under multi-label concept by integrating a convolutional neural network and cellular automata: a case study of Huizhou China. Gisci Remote Sens 59(1):609–632

Yang Y, Liu Y, Li Y, Du G (2018) Quantifying spatio-temporal patterns of urban expansion in Beijing during 1985–2013 with rural-urban development transformation. Land Use Policy 74:220–230

Zhang N, Chen H, Chen J, Chen X (2016) Social media meets big urban data: a case study of urban waterlogging analysis. Comput Intell Neurosci

Zhongming Z, Linong L, Xiaona Y, Wangqiang Z, Wei L (2020) World cities report 2020: the value of sustainable urbanization

Zope PE, Eldho TI, Jothiprakash V (2016) Impacts of land use–land cover change and urbanization on flooding: a case study of Oshiwara River Basin in Mumbai, India. CATENA 145:142–154